An Automatic Plant Disease Symptom Segmentation Concept Based on Pathological Analogy

*Aliyu Muhammad Abdu
School of Electrical Engineering
University Technology Malaysia,
81310 Johor, Malaysia
Email: aliyu104@yahoo.com

Musa Mohd Mokji
School of Electrical Engineering
University Technology Malaysia,
81310 Johor, Malaysia
musamm@utm.my

Usman Ullah Sheikh
School of Electrical Engineering
University Technology Malaysia,
81310 Johor, Malaysia
usman@fke.utm.my

***Abstract*— This paper proposes an automatic disease symptom segmentation algorithm using a simple pathological pattern recognition concept to segment plant disease visual symptoms on digital leaf images. The novelty of the algorithm is in the use of pathological analogy of diseases caused by pathogens, distinct homogeneous patterns relative to the disease progression, to segment individual images into symptomatic, necrotic, and blurred regions. Applying the pathological concept allow for actual disease lesion areas to be quantized in accordance with their true analogy. As a result, individual pattern characteristics of each lesion along the leaf surface can be tracked and features can later be extracted for characterization using machine learning. By employing the concept, the proposed algorithm applies a fusion of simple color space manipulation HSV and CIElab with deltaE (ΔE) color relativity equation to compute each lesion type pixels color. The obtained results are encouraging, successfully localizing and quantifying individual disease lesions. This also indicates the applicability of the proposed approach in discriminating plant diseases based on their analogical dissimilarity. Moreover, it provides opportunities for early identification and detection of fine changes in plant growth, disease stage and severity estimation to assisting crop diagnostics in precision agriculture.**

Keywords*— *Pattern analysis, pathological analogy, Segmentation, Plant disease lesion, Plant disease detection

I. INTRODUCTION

A. Background

Ssegmentation of disease lesion area is a crucial step in the application of machine learning for disease incidence detection and severity estimation [3-5]. Various computer-aided segmentation approaches exist categorized as: 1) manual when every time the user must tune one or several parameters in the software to achieve the segmentation [6], 2) semi-automatic where user manually initializes the segmentation which then proceeds automatically [7], or 3) automatic where no intervention by the user other than submitting the image to be analyzed [2, 8]. Each segmentation process has a limited number of stages ranging from 2 to 3. The first stage normally involves separating the leaf (foreground) from other surrounding areas (background) of the image. The second stage, referred to as region of interest or ROI segmentation is separating the visible disease lesion region from the leaf [9]. Third step, which has just recently been practiced, is further segmenting the ROI into homogenous color segments [4].

The use of image analysis tools for the measure of plant disease lesion segments at a scale of leaf did not receive much attention until the 1970s and 80s when desktop computers, image analysis software programs and relatively inexpensive digital cameras emerged [10]. It was at that time expert pathologist actively started comparing assessment methods quantitatively. Such early methodologies steered future applications and demonstrated the capacity of advance image analysis to measure disease incidence and severity such as that of Lindow and Webb (1983) and Lindow (1983) [11, 12]. Nowadays plant disease detection using machine learning (ML) has gained tremendous momentum, and with it the necessity to better synergize the machine learning methods with pathological expert systems that originally lay the foundation of plant disease detection [10, 13]; the manual approach from the perspective of plant disease pathological analogy [11, 14].

The general ML process basically involves four stages of which segmentation and subsequent feature extraction are the critical ones that determine the efficiency every learning model [14, 15]. The features would be a collection of redundant patterns of properties that sufficiently portray the quantifiable detail of the target region [14], ROI. Each feature would then quantifiably interpret the disease pattern and in general sense portray the similarity or not between the localized pixels. Absolute majority of the existing methods for disease classification employ the concept of only color homogeneity in segmenting disease lesions. Thus, the criteria for subdivision of lesions were only loosely characterized and largely based on superficiality. This is simply on the perception that healthy tissue is purely green and diseased symptoms are not (another color deviating from purely green). While this may hold true in some disease cases other plant stress such as nutrients deficiency exhibit similar discolorations as some diseases due to the influence of environmental factors [16]. This produces high tendency of segmenting false ROI and ultimately extraction of misleading features. To the best of our knowledge, no reported work segment exceptionally on the concept of pathological analogy. In this regard, this paper proposes a pathological analogy-based segmentation concept to automatically segment 3 disease lesion types

978-1-7281-0755-4/19/$31.00 ©2019 IEEE

symptomatic, necrotic, and blurred regions with a focus on the devastating diseases early and late blight.

B. Early and late blight diseases pathological analogy

Plant disease pathology (or phytopathology) deals with the study of plant diseases from cause to infection, effect, infestation, and control [16]. Plants in both natural and cultivated green houses are always susceptible to diseases largely caused by pathogens of which symptoms of various degrees in the form of lesions manifest. Such lesion areas of disease tissue are generally classified into chlorosis and necrosis counted as number of colonies [17, 18]. Variations in disease lesion characteristics and infection stages are relative to the type of pathogen and the host plant, and each variation exhibits distinct patterns of visible properties [16]. However, a few lesion variations develop similar infection stages cut across multiple plant species such as in the case of vegetable early and late blight caused respectively by Alternaria fungus and the devastating pathogen Phytophthora [19, 20]. The two diseases are among the devastating plant diseases that are recurrent [21, 22] and cause long term loss and damage not only to the crops but to the environment as well .

Early and late blight peculiarly share distinct features this often affect the ability of automated algorithms in providing accurate results but human experts as well [23]. The degree of similarity often also leads to difficult challenges such as resulting to intensive computations that often ended up yielding significant misclassification error. The analogical pattern of EB disease symptom is very similar across the four common hosts (tomato, potato, pepper, and egg-plant). They start with small dark brown or black necrotic spots or lesions which later enlarge forming concentric rings with a bull's-eye pattern surrounded by yellowish (chlorosis) zone [19, 22]. In the case of LB, initial infection symptoms start with small dark lesions often on leaf tips, after which it manifest to dark brown or black water-soaked lesions occasionally with a pale yellowish-green border that fades into the healthy tissue [20, 24]. Both diseases manifest by expanding over the healthy green tissue with a fuzzy zone in-between healthy tissue and disease lesion. Regarding this, each leaf would have 4 regions: leaf healthy tissue that is purely green, leaf symptomatic region (yellowish or green-whitish area), leaf necrotic region (brown or black area), and blurred region in-between healthy and disease lesion. However, it should be noted that the blurred region is not part of disease lesion. It thus follows the characteristic in TABLE I.

TABLE I: DISEASE LESION CHARACTERISTICS FROM PATHOLOGICAL ANALOGY

Disease	***Disease lesion type***	***Pathological characteristics***
Early blight (EB)	Symptomatic	yellowish or yellowish-green zones
	Necrotic	dark brown or black necrotic (concentric) spot(s) or lesions
Late blight (LB)	Symptomatic	water-soaked (whitish) zones. Occasionally containing some yellowish part also
	Necrotic	dark-brown or black spot(s) or lesions

Hence, despite the amount of successes by existing automatic methods, disease assessment through imagery analysis was found in most cases not in close agreement to actual values [25]. Bock *et al.* concluded that vast majority of presented works often gave accurate results in some specific cases, but generally more time consuming even when so [10]. Current image analysis does not offer a direct way of distinguishing actual symptoms localized into necrotic or symptomatic caused by pathogens. With the localized disease lesion segmentation the stage of disease development can be numerically assessed or estimated [26]. This advantage clearly describes the disease development stage and of immense importance to Raters for numerous interpretation such as in plant breeding programs [27] and yield loss estimation [28]. A critical review made by Hughes and madden (1995) [17] and Madden and Hughes (1999) [29] reassessed the methodologies for the analysis of disease particularly concerning aggregated disease patterns such as spatial hierarchy and heterogeneity distribution pointing the potential for error in correlations between experiments and treatments if overlooked. Thus, the novelty target of this work is to pioneer an intelligent blend of the human expert system concept into the computer vision and machine learning techniques. Individual symptomatic (R_S), necrotic (R_N) and blurred (R_B, in-between healthy and disease) regions were identified, segmented and quantified in accordance with pathological analogy.

II. MATERIALS AND METHODS

A. Image dataset

The PlantVillage public image dataset [30] consisting of leaf healthy and diseased (early and late blight) images was utilized along with other images collected from the internet to compensate for pepper blight images. A detail breakdown of image data is given in TABLE II. This data was chosen as the diseases highlighted peculiar disease anatomy factor where symptom pattern regions are not always palpable. Furthermore, early and late blight disease symptoms exhibit similar symptoms across the solanaceous vegetable crops [22, 31, 32] including the 3 considered in this research. In this regard, they are most often difficult to characterize. The whole dataset was spilt, randomly for each class (late blight – LB, early blight – EB) into two groups as training and testing to allow for proper assessment of characterization features. All the images for the three classes are of the same scale size of 256×256.

B. Methodology

It has been established that in comparison to blue and red are of healthy tissue [9]. The study also presented an automatic extended region of interest (EROI) segmentation to incorporate, by extending the border region, blurred zones (blurred tissue) using color homogeneity thresholding [9]. Part of that methodology is being used here.

1) EROI segmentation

In this step, healthy tissue pixels exhibiting higher deviations towards the green hue are masked using our already established EROI segmentation algorithm [9]. Pixels of the healthy green tissue are masked based on the computed ration of green color to red and blue except for

TABLE II. DISEASE LESION LOCALIZATION ACCORDING TO PATHOLOGICAL ANALOGY ON HOST SPECIE

Disease Lesion Type	***Symptom analogy***	***Vegetable specie***	***N0. of samples per specie***	***Sample image***	
				Original	***EROI***
Symptomatic	yellowish-green or water-soaked zones	Potato, tomato, and pepper	Potato = 500 Tomato = 500 Pepper = 30		
Necrotic	dark-brown or black zones				
Blur	Fuzzy zone (in between symptomatic/necrotic and healthy)				

those within the computed extended region to cover blurred region (containing symptom progression information). On this basis, threshold values were set between four pixels groups to generate 4 masks and then combined to form the final segmentation mask leaving only the EROI [9]. The EROI represented as I_{EROI} is then a combination of the three such that:

$$I_{EROI}(x,y) = R_S(x,y) + R_N(x,y) + R_B(x,y) \quad (1)$$

Where R_S is symptomatic region comprising of yellowish and water-soaked zones, R_N necrotic region for dark brown or black, and R_B blurred region (in-between healthy and symptomatic).

2) Segmentation of disease lesion types

To analyze and segment individual diseased segments, the EROI image is transformed from RGB to CIE L*a*b* and HSV color spaces [33]. Both were considered in this study as they were designed to be perceptually uniform with respect to the way humans visually perceive color. The steps are as follows:

- Compute and create initial reference seed regions.
- Compute color difference between seed region and input image to generate masks.
- Apply masks individually to acquire lesions types using ΔE.

To compute seed regions the process starts by obtaining individual representative threshold ranges, following the EB disease analogy, for *H-channel* and *a-channel* as $low_i \leq t_i < high_i$ for R_N and R_S of each disease. The thresholds are applied to create the seed bounding region B as:

$$B_j(R_j) = \begin{cases} 1 & t_{Htl} \leq P(x,y) \leq t_{Hth} \\ 0 & otherwise \end{cases} \quad (2)$$

$$B_j(R_j) = \begin{cases} 1 & t_{atl} \leq P(x,y) \leq t_{ath} \\ 0 & otherwise \end{cases} \quad (3)$$

Where $j = N, S$ represents necrotic and symptomatic respectively and $P(x,y)$ individual pixels.

Then, computing the $L^*a^*b^*$ color difference with $B_j(R_j)$ as reference is done as:

$$\Delta L^*a^*b^* = \begin{cases} \Delta L_j = L_1 - L_2 \\ \Delta a_j = a_1 - a_2 \\ \Delta b_j = b_1 - b_2 \end{cases} \quad (4)$$

Where L_1, a_1, b_1 are channels of I_{EROI}, and L_2, a_2, b_2 are of $B_j(R_j)$. The color differences are computed as ΔE [34]:

$$\Delta E_j = \sqrt{\Delta L_j^2 + \Delta a_j^2 + \Delta b_j^2} \quad (5)$$

The final masks segmenting pixels belonging to R_N and $R_S$are acquired by:

$$P_1(x,y) = \{(x,y) \in I_{EROI} | \Delta E_{j1}(x,y)\} \quad (6)$$

$$P_2(x,y) = \{(x,y) \in I_{EROI} | \Delta E_{j2}(x,y)\} \quad (7)$$

Where P_1 segments R_N and R_S for EB and P_2 for those of LB. $p_N(x,y)$, $p_S(x,y)$ are pixels of necrotic and symptomatic regions respectively.

Blur region pixels would then be:

$$P_B(x,y) = I_{EROI}(x,y) - \{P_1(x,y) + P_2(x,y)\} \quad (8)$$

Equations (6), (7), and (8) are used to localize each disease lesion region (example Fig. 1).

C. Data analysis and Validation of the prosed algorithm

Despite the inability to ground-truth boundaries due to subjectivity, it is deemed important to obtain a measure of the algorithm's performance. Though removing subjectivity from such manual segmentation process is impossible [2], care was taken to reduce it to the barest minimum. Thus, the pixels of each of the lesion colonies were manually labelled and segmented by an expert.

All the data analysis was carried out using MATLAB R2017b (The MathWorks Inc., Natick, MA) program. Using the manual measurements as the ground truth, the following were calculated: the percentage of missed disease lesion pixels in each category (false negatives, FN and false positives, FP), and the percentage of missed blurred pixels (SB). The first two statistics represent error in measurement, while the third statistic demonstrates the general behavior of the algorithms in dealing with the blurred regions. Also, comparison was made with the

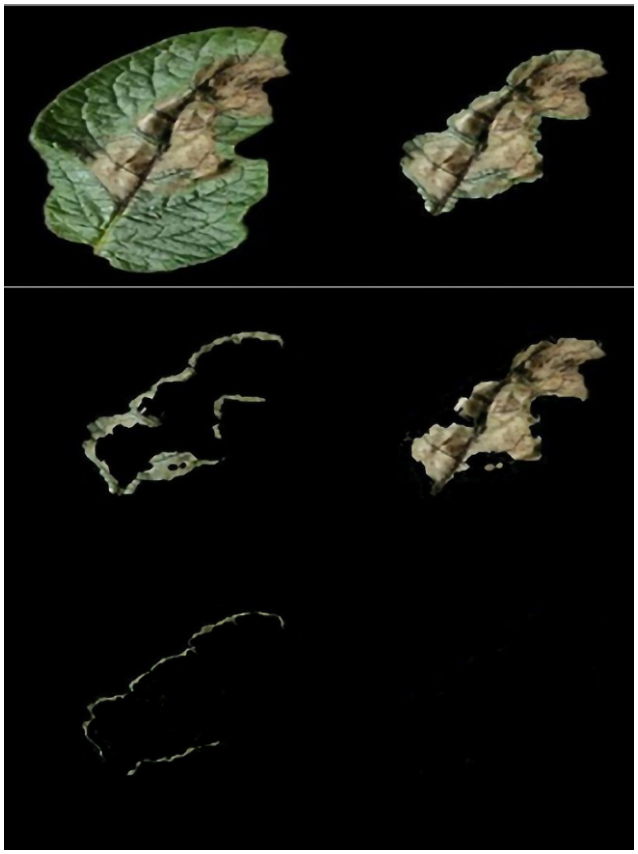

Fig. 1: Steps in the algorithm for localizing disease lesion colonies. The leaf sample is that of a potato infected with late blight.

results yielded by the proposed algorithm with two other segmentations methods that considered homogeneity.

The distribution of error N_e for each of the localized regions that indicates the magnitude of error expected in each case was calculated as N_d/N_T, where N_d is the number of pixels misclassified, and N_T is the total number of pixels in the leaf. The recall also known as true positive rate was computed as $TP/(TP + FN)$ where TP and FN are true positive and false negative rates. This also reflects the performance of the proposed algorithm in accurately classifying lesion pixels.

III. Results

TABLE III presents the segmentation performance of the proposed algorithm in accordance with the 3 disease lesion regions. The proposed algorithm was consistently more accurate when compared with the other two techniques: not only were the error rates lower in all disease categories, but the proposed algorithm was the only method that was consistently robust quantifying disease lesion from the lesion colonies.

The results (TABLE III) show FP of the proposed method is lower (0.35% to 1.33%) in all lesion categories compared to Camargo's (1.20% to 1.51%) and is within close uniformity with Barbedo's (0.51% to 1.40%), though slightly higher. The proposed algorithm is more robust in characterizing symptomatic and necrotic regions from the blurred as indicated by FN (0.8% to 4.4%) compared to the other two (5.3% to 7.3%). The proposed algorithm also shows a significant decrease by no less than 80% in the proportion of pixels missed in the blurred region classified as symptomatic or necrotic (3.6% to 15.2%) compared to the other two algorithms (91.5% to 97.2%) and (60.1% to 92.4%). Though the ratio of the blurred region in relation to disease lesion size is small ranging from 5% to 22%, its significance cannot be underrated considering it will provide vital information about the disease progression and severity.

The true positive rate (TP, TABLE IV) indicated the performance of the algorithm in accurately localizing the disease lesion pixels into symptomatic and necrotic regions. Having an average accuracy of 96.2%, the algorithm outperforms the other two which stood at 92.8% and 94.6%.

TABLE IV. True Positive Rate (TP) Of The Proposed Algorithm, Comparing With Two Other Methods

Method	**Camargo and Smith**		**Barbedo**		**Proposed**	
Disease lesion region	***S***	***N***	***S***	***N***	***S***	***N***
TP	92.8%	92.7%	94.4%	94.7%	94.6%	97.8%

IV. Discussion

The success of the proposed algorithm is partly featured to the EROI segmentation [9] as it accurately captures the border region between blurred and healthy tissue. However, two main sources of error were the most frequent causes of FPs and FNs. The first is due to their nature of not always having pronounced diseased border. The blurred region, particularly for late blight disease, often have several pixels that should have been included in either the healthy tissue or symptomatic region in the ground truth. This explains the slightly high proportion of pixels (15.2%) identified by the algorithm as symptomatic. Despite this nature, the algorithm was able to lower the error rate (N_e, 2.8% to 0.6%) as opposed to other existing methods (Camargo and Smith, 4.3% to 4.2%; and Barbedo, 3.0% to 2.9%). The second error was in leaves with early stages of infection have characteristically small symptom units and are less pronounced, references (presumed actual values measured by the expert) may not be entirely accurate which in turn made those distortions a bigger source of error. Other source of error was because of isolated outlier pixels

TABLE III. Summary Of Segmentation Performance (in % of cases in each class) Of The Proposed Algorithm. *FP, FN*, Represent Missed Disease Lesion Pixels, *SB* Represent Missed Blurred Pixels, And NE Distribution Of Error

Result Summary	**Camargo and Smith [1]**				**Barbedo [2]**				**Proposed**			
Lesion Region	***FP***	***FN***	***SB***	***N_e***	***FP***	***FN***	***SB***	***N_e***	***FP***	***FN***	***SB***	***N_e***
Symptomatic	1.51	7.2	94.0	4.2	1.40	5.6	91.0	3.0	1.33	4.4	15.2	2.8
Necrotic	1.20	7.3	91.5	4.3	0.51	5.3	92.4	2.9	0.35	1.8	03.6	0.6

that, despite being part of the symptomatic region, have characteristics more closely related to the fuzzy zone.

The overall performance of the proposed algorithm indicated great promise in having a complete hybrid automatic system for plant disease detection, incorporating intelligent analogy of diseases.

V. CONCLUSION

The main contribution of this paper is on applying pathological concept of identifying visual symptoms in automatically identifying and segmenting plant disease lesion types. The proposed algorithm is simple to implement, being based on the arithmetic manipulation and computation of color channels relativity designed to be perceptually uniform with respect to the way humans visually perceive color. Compared with other segmentation works, the results indicate that the algorithm performs incredibly well outperforming the others in localizing symptomatic, necrotic, and blurred disease lesion regions. This substantiate the superiority of the proposed algorithm in localizing the three lesion colonies in accordance with the disease's analogies as a pioneer of an intelligent blend of human expert system concept of plant disease analogy with the computer vision and machine learning techniques.

ACKNOWLEDGMENT

The authors thank the Ministry of Education Malaysia and Universiti Teknologi Malaysia (UTM) for their support under the University Grant (UTM Flagship). Grant number PY/2018/02995 under project title: Distorted Images Pre-processing for Deep Neural Network Classification.

REFERENCES

[1] A. Camargo and J. Smith, "An image-processing based algorithm to automatically identify plant disease visual symptoms," *Biosystems engineering,* vol. 102, no. 1, pp. 9-21, 2009.

[2] J. G. A. Barbedo, "A new automatic method for disease symptom segmentation in digital photographs of plant leaves," *European journal of plant pathology,* vol. 147, no. 2, pp. 349-364, 2017.

[3] J. G. A. Barbedo, "A review on the main challenges in automatic plant disease identification based on visible range images," *Biosystems Engineering,* vol. 144, pp. 52-60, 2016.

[4] G. Dhingra, V. Kumar, and H. D. Joshi, "A novel computer vision based neutrosophic approach for leaf disease identification and classification," *Measurement,* vol. 135, pp. 782-794, 2019/03/01/ 2019.

[5] E. Hossain, M. F. Hossain, and M. A. Rahaman, "A Color and Texture Based Approach for the Detection and Classification of Plant Leaf Disease Using KNN Classifier," in *2019 International Conference on Electrical, Computer and Communication Engineering (ECCE)*, 2019, pp. 1-6: IEEE.

[6] S. J. Pethybridge and S. C. Nelson, "Leaf Doctor: A new portable application for quantifying plant disease severity," *Plant Disease,* vol. 99, no. 10, pp. 1310-1316, 2015.

[7] G. Cerutti, L. Tougne, J. Mille, A. Vacavant, and D. Coquin, "Understanding leaves in natural images–a model-based approach for tree species identification," *Computer Vision and Image Understanding,* vol. 117, no. 10, pp. 1482-1501, 2013.

[8] M. Rico-Fernández, R. Rios-Cabrera, M. Castelán, H.-I. Guerrero-Reyes, and A. Juarez-Maldonado, "A contextualized approach for segmentation of foliage in different crop species," *Computers and Electronics in Agriculture,* vol. 156, pp. 378-386, 2019.

[9] A. M. Abdu, Mokji M.; Sheikh, U. U, "An Investigation into The Effect of Disease Symptoms Segmentation Boundary Limit on Classifier Performance in Application Of Machine Learning for Plant Disease Detection," *International Journal of Agricultural, Forestry & Plantation (ISSN No: 2462-1757)* Journal vol. 7, no. 6, pp. 33 - 40, December 2018, Art. no. IJAFP_39.

[10] C. Bock, G. Poole, P. Parker, and T. Gottwald, "Plant disease severity estimated visually, by digital photography and image analysis, and by hyperspectral imaging," *Critical Reviews in Plant Sciences,* vol. 29, no. 2, pp. 59-107, 2010.

[11] S. Lindow, "Estimating disease severity of single plants," *Phytopathology,* vol. 73, no. 11, pp. 1576-1581, 1983.

[12] S. Lindow and R. Webb, "Quantification of foliar plant disease symptoms by microcomputer-digitized video image analysis," *Phytopathology,* vol. 73, no. 4, pp. 520-524, 1983.

[13] A. Singh, B. Ganapathysubramanian, A. K. Singh, and S. Sarkar, "Machine learning for high-throughput stress phenotyping in plants," *Trends in plant science,* vol. 21, no. 2, pp. 110-124, 2016.

[14] K. Mochida *et al.*, "Computer vision-based phenotyping for improvement of plant productivity: a machine learning perspective," *GigaScience,* vol. 8, no. 1, p. giy153, 2018.

[15] S. Kaur, S. Pandey, and S. Goel, "Plants Disease Identification and Classification Through Leaf Images: A Survey," *Archives of Computational Methods in Engineering,* journal article January 19 2018.

[16] G. N. Agrios, *Plant Pathology*, 5th ed. Elsevier Science, 2005, p. 952.

[17] L. Madden and G. Hughes, "Plant disease incidence: distributions, heterogeneity, and temporal analysis," *Annual Review of Phytopathology,* vol. 33, no. 1, pp. 529-564, 1995.

[18] P. S. Ojiambo, J. Yuen, F. van den Bosch, and L. V. Madden, "Epidemiology: Past, Present, and Future Impacts on Understanding Disease Dynamics and Improving Plant Disease Management—A Summary of Focus Issue Articles," *Phytopathology,* vol. 107, no. 10, pp. 1092-1094, 2017/10/01 2017.

[19] R. Chaerani and R. E. Voorrips, "Tomato early blight (Alternaria solani): the pathogen, genetics, and breeding for resistance," *Journal of general plant pathology,* vol. 72, no. 6, pp. 335-347, 2006.

[20] M. Nowicki, E. U. Kozik, and M. R. Foolad, "Late blight of tomato," *Translational genomics for crop breeding,* vol. 1, pp. 241-265, 2013.

[21] W. Fry, "Phytophthora infestans: the plant (and R gene) destroyer," *Molecular plant pathology,* vol. 9, no. 3, pp. 385-402, 2008.

[22] R. D. Rands, *Early blight of potato and related plants*. Agricultural Experiment Station of the University of Wisconsin, 1917.

[23] L. V. Madden, G. Hughes, and F. v. d. Bosch, *The study of plant disease epidemics*. St. Paul: American Phytopathological Society (APS Press), 2007, p. xiv + 421 pp.

[24] W. E. Fry and S. B. Goodwin, "Re-emergence of potato and tomato late blight in the United States," *Plant Disease,* vol. 81, no. 12, pp. 1349-1357, 1997.

[25] T. U. Rehman, M. S. Mahmud, Y. K. Chang, J. Jin, and J. Shin, "Current and future applications of statistical machine learning algorithms for agricultural machine vision systems," *Computers and Electronics in Agriculture,* vol. 156, pp. 585-605, 2019/01/01/ 2019.

[26] W. Turechek and L. Madden, "A generalized linear modeling approach for characterizing disease incidence in a spatial hierarchy," *Phytopathology,* vol. 93, no. 4, pp. 458-466, 2003.

[27] F. W. Nutter and P. D. Esker, "The role of psychophysics in phytopathology: The Weber–Fechner law revisited," *European Journal of Plant Pathology,* vol. 114, no. 2, pp. 199-213, 2006.

[28] E. C. Oerke, "Crop losses to pests," *The Journal of Agricultural Science,* vol. 144, no. 1, pp. 31-43, 2006.

[29] L. Madden and G. Hughes, "An effective sample size for predicting plant disease incidence in a spatial hierarchy," *Phytopathology,* vol. 89, no. 9, pp. 770-781, 1999.

[30] S. P. Mohanty, D. P. Hughes, and M. Salathé, "Using deep learning for image-based plant disease detection," *Frontiers in plant science,* vol. 7, p. 1419, 2016.

[31] W. L. Morris and M. A. Taylor, "The Solanaceous Vegetable Crops: Potato, Tomato, Pepper, and Eggplant A2 - Thomas, Brian," in *Encyclopedia of Applied Plant Sciences (Second Edition)*, B. G. Murray and D. J. Murphy, Eds. Oxford: Academic Press, 2017, pp. 55-58.

[32] P. Padmanabhan, A. Cheema, and G. Paliyath, "Solanaceous Fruits Including Tomato, Eggplant, and Peppers," in *Encyclopedia of Food and Health*Oxford: Academic Press, 2016, pp. 24-32.

[33] M. D. Fairchild, *Color appearance models*. John Wiley & Sons, 2013.

[34] A. R. Robertson, "The CIE 1976 color - difference formulae," *Color Research & Application,* vol. 2, no. 1, pp. 7-11, 1977.